

Drought analysis based on precipitation generation from GCMs for the Qingjiang River Basin

KUNXIA YU, LIHUA XIONG, LEIHUA DONG & MIN WAN

*State Key Laboratory of Water Resources and Hydropower Engineering Science, Wuhan University,
Wuhan 430072, China*

xionglh@whu.edu.cn

Abstract This paper aims to assess model reliability of 21 global climate models (GCMs) to reproduce observed historical monthly rainfall and drought, especially extreme events over Qingjiang River Basin. Monthly areal precipitation series were downscaled from 21 GCMs using the Statistical DownScaling Model (SDSM). All the downscaling rainfalls were evaluated against the 1960–1999 observed rainfall data over Qingjiang River Basin. The main conclusions include: (a) most downscaled rainfalls can reasonably reproduce the observed monthly areal rainfall series in both calibration period and validation period, although downscaled rainfall time series are more stationary; (b) downscaled rainfalls perform poorly when they come to drought, and observed drought characteristics cannot be well reproduced, but category simulation accuracy is generally satisfactory to some degree; (c) there is no clear difference in the ability to produce historical rainfall characteristics between GCMs, but the difference in the capability to simulate droughts and extreme events is significant.

Key words precipitation; drought; extreme; downscaling; global climate models; Qingjiang River Basin

INTRODUCTION

Extreme event risk is highly topical in water resource management since it is associated with severe damage to social and economic development. The increasing frequency and intensity of extreme events have a potential link with climate change (Frich *et al.*, 2002; Nicholls & Alexander, 2007). A global climate model (GCM) is an advanced tool to estimate future climate change scenarios. Assessing model reliability is meaningful to investigate future climate change scenarios to predict a potential extreme event.

Twenty-four GCMs are available to simulate climate change scenarios in the future. In many studies rainfall downscaled from some GCMs for current climate is compared with the observed historical rainfall to assess model reliability (Whitehead *et al.*, 2006; Perkins *et al.*, 2007; Chiew *et al.*, 2009, 2010; Timbal *et al.*, 2009). This paper assesses the relative abilities of the 21 GCMs used in the IPCC AR4 (IPCC, 2007) to reproduce historical observed monthly rainfall and drought, especially extreme events in the Qingjiang River Basin, a main branch in the middle Yangtze River Basin near the Three Gorges Project area.

Downscaling work is a prerequisite because the output of GCMs is too coarse for a hydrological region. Various downscaling models have been developed; one popularly used is the Statistical DownScaling model (SDSM) (Wilby *et al.*, 2002; Harpham & Wilby, 2005; Khan *et al.*, 2006). It was used to generate downscaled precipitation in this study. The choice of predictor variables is critical in capturing the anthropogenic climate change signal in the GCM (Hewitson & Crane, 1996; Cavazos & Hewitson, 2005). Principal component analysis (PCA) of the predictor field is the most common technique (Zorita *et al.*, 1995; Ghosh & Mujumdar, 2008); it was applied to establish a suitable set of input variables used as the inputs into SDSM.

Hence, there are 21 different precipitation generation results in total. All the downscaling rainfalls are evaluated against the 1960–1999 observed rainfall data over Qingjiang River Basin to assess model reliability of the 21 GCMs used in the IPCC AR4 to reproduce the observed historical rainfall and drought, especially extreme events over Qingjiang River Basin.

STUDY AREA AND DATA

The 16 700 km² Qingjiang River Basin is located in the middle reach of Yangtze River Basin in the central part of China, between 29°33′–30°50′N and 108°35′–111°35′E. Qingjiang River is a mother

river with long history human habitation and agricultural development. The climate belongs to typically subtropical monsoon climate, warm and wet. The average annual temperature is 15–16°C, average annual relative humidity is 80–84%, and average annual precipitation and evaporation are 1460 mm and 600–800 mm, respectively. The terrain of Qingjiang River Basin is intensely variable, from the western high mountains to low altitude hills to the east, as shown in Fig. 1.

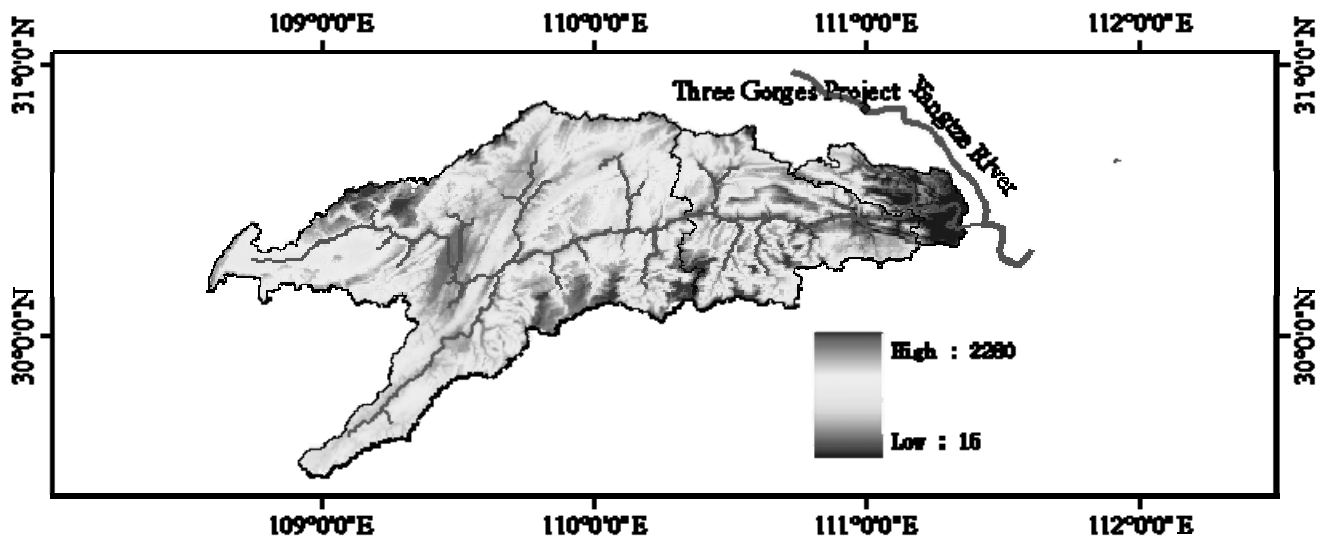


Fig. 1 Geographic location of Qingjiang River Basin.

The predictand to be downscaled is monthly precipitation. Observed rainfall data is areal mean precipitation over Qingjiang River Basin from 1960 to 1999. The calibration period is 1960–1989 and the validation period is 1990–1999. Atmospheric predictor data used to calibrate downscaling methods come from the WCRP CMIP3 multi-model database (<https://esgcet.llnl.gov>). The 17 candidate predictors considered are relative humidity at 500 and 850 hPa, specific humidity at 500 and 850 hPa, surface specific humidity, mean sea level pressure, surface air temperature, zonal wind component at 500 and 850 hPa, zonal surface wind speed, meridional wind component at 500 and 850 hPa, meridional surface wind speed, omega at 500 and 850 hPa and geopotential heights at 500 and 850 hPa.

GCM DOWNSCALED RAINFALL RESULTS

Twenty-one suitable sets of input variables chosen from 21 GCMs by applying PCA techniques were used as the inputs into SDSM to downscale precipitation over the Qingjiang River Basin. The rainfalls downscaled from 21 GCMs were compared with observed rainfall in various ways to evaluate their performance comprehensively. Locally weighted scatterplot smoothing (LOWESS) curves (Fig. 2) were used to explore local regularities and trends between observed and downscaled rainfalls; objective functions (Table 1) to compare statistics of various rainfall characteristics; box plots (Fig. 3) to represent downscale accuracy of monthly rainfall, and SPI (Fig. 4) to analyse drought characteristics.

LOWESS is an effective tool to explore the relation between two variables (Cleveland, 1979; Cleveland & Devlin, 1988). At each point in the data set a low-degree polynomial is fitted to a subset of the data, with explanatory variable values near the point whose response is being estimated. The polynomial is fitted using weighted least squares, giving more weight to points near the point whose response is being estimated and less weight to points further away.

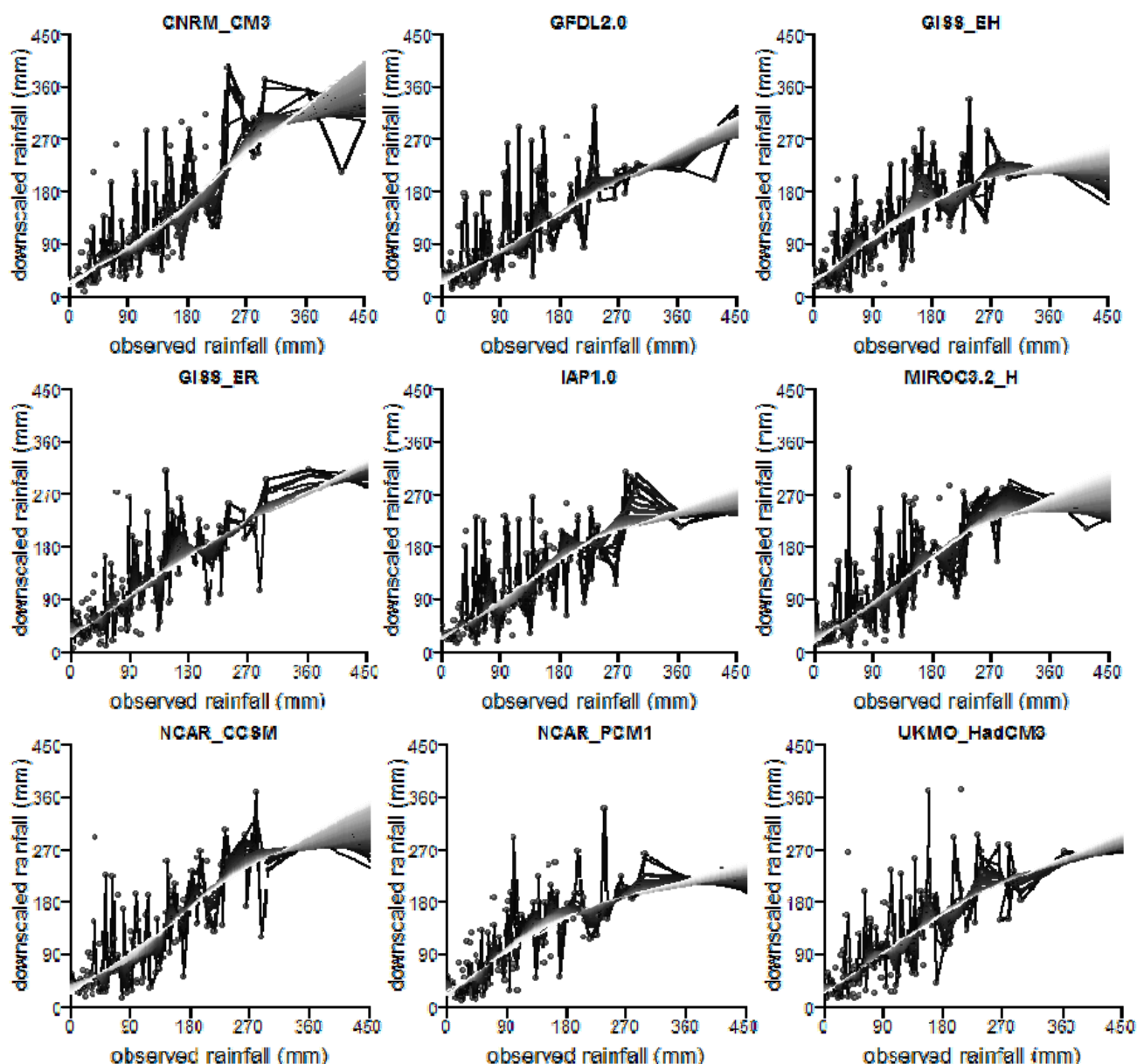


Fig. 2 LOWESS curves of observed rainfall against downscaled rainfalls from some typical GCMs over the validation (1990–1999) period.

Table 1 Summary statistics comparing observed rainfall characteristics with downscaled rainfalls over validation period (1990–1999).

GCMs	RMSE (mm)	<i>r</i>	NSE	<i>d</i>	GCMs	RMSE (mm)	<i>r</i>	NSE	<i>d</i>
BCCR-BCM2.0	65.5	0.69	0.45	0.82	INM-CM3.0	61.9	0.74	0.51	0.85
CGCM3.1(T47)	67.8	0.67	0.42	0.81	MIROC3.2-H	67.3	0.70	0.42	0.83
CGCM3.1(T63)	69.2	0.71	0.39	0.84	MIROC3.2-M	69.5	0.64	0.39	0.78
CNRM-CM3	63.2	0.76	0.49	0.87	MIUB	65.4	0.70	0.46	0.83
GFDL 2.0	62.7	0.72	0.50	0.84	MPI-ECHAM5	62.7	0.73	0.50	0.84
GFDL 2.1	63.7	0.76	0.48	0.87	MRI	66.0	0.71	0.45	0.84
GISS-AOM	70.1	0.68	0.38	0.82	NCAR-CCSM	63.0	0.74	0.50	0.86
GISS-EH	65.9	0.69	0.45	0.82	NCAR-PCM1	61.9	0.72	0.51	0.84
GISS-ER	61.6	0.74	0.52	0.85	UKMO-HadCM3	65.9	0.71	0.45	0.84
IAP1.0	65.2	0.70	0.46	0.83	UKMO-HadGEM1	66.3	0.69	0.44	0.83
INGV	66.5	0.69	0.44	0.82	Median	65.5	0.71	0.45	0.84

Figure 2 shows the relation between observed and downscaled rainfalls from some typical GCMs over the validation period. In the plot the robust smoothed value of LOWESS curves ranged from 0.01 to 1 to explore local regularities and trends between observed and simulated rainfall. The lighter the colour is, the closer robust smoothed value goes to 1, and more data are involved in one smoothed window. As shown in Fig. 2, the slope of most regression curves is less than 1, and the terminal of regression curves greatly deviate from the regression line, with downward trends for most simulations. It is illustrated that most downscaled rainfalls underestimate the observed, especially extreme rainfall. Only a few GCMs perform well, such as CNRM-CM3 and NCAR-CCSM. There is not much difference between downscaled rainfalls in general, but the difference in the ability to reproduce extreme rainfall between GCMs is significant.

Table 1 summarises the comparative statistics of various rainfall characteristics: (a) root mean square error (RMSE) between observed and downscaled monthly rainfalls; (b) linear correlation (r) of downscaled monthly rainfalls *versus* observed; (c) Nash-Sutcliffe efficiency (NSE) to characterise the agreement between the two monthly rainfall distributions; (d) index of agreement d to gauge downscaled rainfall performance. Index of agreement is a normalized measure of sum of squared errors developed to overcome the sensitivity of correlation-based statistics to discrepancies between the observed and modelled means and variance (Willmott, 1982).

Downscaled rainfalls generally have good agreement with observed rainfall and can reproduce the observed monthly rainfall temporal patterns, as indicated by the generally greater than 0.8 index of agreement and 0.7 linear correlations. However, differences still exist between rainfall downscaled from GCMs and observed rainfall. Most of the downscaled results cannot adequately reproduce observed monthly rainfall distribution, as indicated by the relatively low NSE values; the median RMSE is 65 mm, about half of the mean monthly rainfall across the study area.

The GCMs can be ranked based on their abilities to reproduce the observed monthly rainfall, but apart from several GCMs with very low NSEs (for example, CGCM3.1 (T63), GISS-AOM, and MIROC3.2-M), there is no clear threshold in the distribution of RMSE, NSE, linear correlation and index of agreement values to separate the better and poorer GCMs (Table 1).

Figure 3 shows the box-whisker plots representing the downscaling accuracy of monthly mean rainfall over calibration period and validation period. In general, the monthly mean rainfall is well simulated in June and July, overestimated in August, and underestimated in other months. This figure also shows the uncertainty range of downscaled rainfall with respect to GCMs. It is smaller during the winter and spring periods than summer and autumn. Uncertainty range is less in the calibration period than validation period, but the ability to reproduce observed rainfall is generally comparable.

DROUGHT SIMULATION RESULTS

Drought causes huge losses in agriculture and damages natural ecosystems; it has received special attention in water resource management. The most robust and effective drought index is the

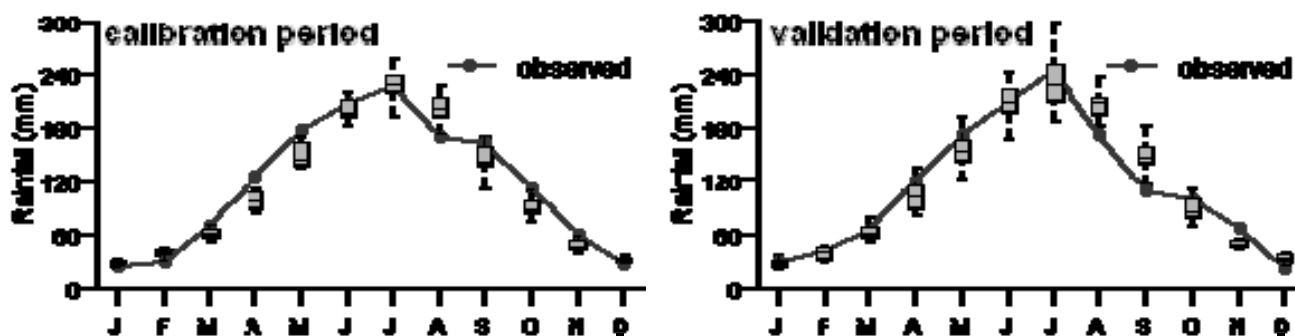


Fig. 3 Observed and downscaled monthly precipitation amounts over the calibration (1960–1989) and the validation (1990–1999) periods. Downscaled monthly rainfall of 21GCMs is given as box plots giving median, upper and lower quartiles and max. and min. values.

Standardized Precipitation Index (SPI), which was developed by McKee *et al.* (1993). The SPI allows the determination of duration, magnitude and intensity of droughts. SPI at 12 months is considered a hydrological drought index, since it is used for monitoring surface water resources. In this research, SPI at 12 months (SPI12) is investigated to estimate the ability of downscaled rainfall to simulate drought. A drought event occurs any time the SPI is continuously negative and reaches an intensity of -1.0 or less. The event ends when the SPI becomes positive.

Figure 4 represents the simulation of SPI12 based on validation period. This figure shows the uncertainty range of SPI12 with respect to GCMs. In general, the simulation is remarkably dramatic. SPI12 of most downscaled rainfalls are very different from the corresponding observed rainfall. The uncertainty range with respect to GCMs is quite wide, but a majority of downscaled rainfalls belong to the Near Normal category with SPI12 value between -0.99 and $+0.99$ according to the classification scale for SPI values (Table 2) (Edward & McKee, 1997). It illustrates that downscaled rainfall time series are more stationary. Most downscaled results did not reproduce observed drought events, especially the extreme drought phenomenon in 1992 and 1993.

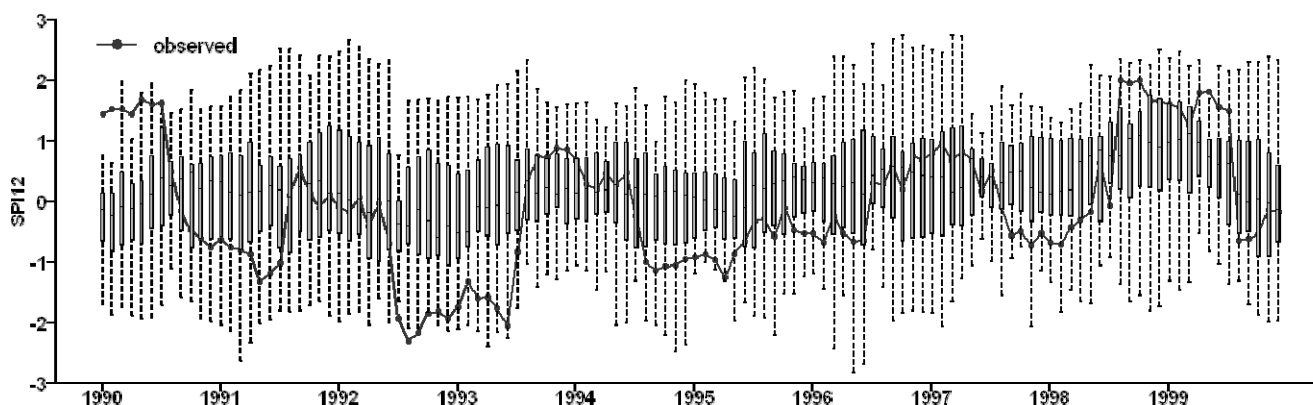


Fig. 4 SPI12 of observed and downscaled rainfall series over the validation (1990-1999) period. SPI12 of 21GCMs is given as box plots.

Table 2 Classification scale for SPI values.

SPI Values	Category	SPI values	Category
$\geq +2.00$	Extremely wet	≤ -2.00	Extremely dry
+1.50 to +1.99	Very wet	-1.50 to -1.99	Severely dry
+1.00 to +1.49	Moderately wet	-1.00 to -1.49	Moderately dry
-0.99 to +0.99	Near normal		

Table 3 summarises the comparative statistics of SPI12 of downscaled rainfalls *versus* observed rainfall: Category Simulation Accuracy (CSA), linear correlation (r), Nash-Sutcliffe efficiency (NSE) and index of agreement (d) to evaluate the ability of downscaled rainfalls to reproduce observed hydrological droughts. Category simulation accuracy is the percent of downscaled rainfalls which are distinguished by same category with observed rainfall based on SPI12.

The category simulation accuracy is reasonable, as indicated by CSA mostly greater than 60%. However, generally lower linear correlation, Nash-Sutcliffe efficiency, and index of agreement values mean that most downscaled results cannot accurately reproduce observed hydrological droughts. The ability to reproduce hydrological droughts is comparable in the calibration period and validation period in general, while the uncertainty range with respect to GCMs is less in the calibration period.

Table 3 Summary statistics comparing SPI12 of observed rainfall with downscaled rainfalls over validation period (1990–1999).

GCMs	CSA (%)	<i>r</i>	NSE	<i>d</i>	GCMs	CSA (%)	<i>r</i>	NSE	<i>d</i>
BCCR–BCM2.0	57.5	−0.19	−1.35	0.33	INM–CM3.0	62.5	0.11	−0.79	0.48
CGCM3.1(T47)	65.0	0.32	−0.49	0.61	MIROC3.2–H	70.0	0.49	0.06	0.71
CGCM3.1(T63)	61.7	−0.09	−1.39	0.31	MIROC3.2–M	64.2	−0.06	−1.18	0.38
CNRM–CM3	56.7	−0.02	−1.12	0.44	MIUB	59.2	0.55	−0.25	0.70
GFDL 2.0	75.8	0.14	−0.52	0.49	MPI–ECHAM5	62.5	0.15	−0.64	0.49
GFDL 2.1	58.3	0.47	−0.15	0.67	MRI	60.8	−0.35	−1.64	0.20
GISS–AOM	56.7	0.21	−0.70	0.52	NCAR–CCSM	70.8	0.08	−0.87	0.36
GISS–EH	70.0	−0.09	−1.41	0.34	NCAR–PCM1	55.8	0.59	0.09	0.76
GISS–ER	52.5	0.25	−0.85	0.54	UKMO–HadCM3	71.7	0.34	−0.54	0.55
IAP1.0	60.8	0.07	−0.79	0.44	UKMO–HadGEM1	66.7	0.21	−0.78	0.53
INGV	58.3	0.31	−0.65	0.56	Median	61.7	0.15	−0.78	0.49

DISCUSSION AND CONCLUSIONS

This paper assesses the relative abilities of the 21 GCMs used in the IPCC 4AR to simulate various 1960–1999 observed rainfall and drought characteristics, and explores how the choice of GCMs used in a study can influence downscaled results using data from a 16 700 km² region over Qingjiang Basin. The results indicate that most downscaled rainfalls have good agreement with the observed rainfall, and can reproduce the observed linear mean monthly rainfall temporal pattern. However, the downscaled rainfall time series are more stationary than the observed. Downscaled rainfalls have poor ability to reproduce monthly rainfall distribution with relatively low NSEs and high RMSEs; most of downscaled rainfalls underestimate the observed, especially extreme rainfall.

Most downscaled results perform poorly when they come to drought. Lower linear correlation, Nash–Sutcliffe efficiency and index of agreement values show that observed drought characteristics cannot be well reproduced, but category simulation accuracy is generally satisfactory to some degree.

Although there is no clear difference in the ability to reproduce historical rainfall characteristics between GCMs, LOWESS plot and SPI12 show that the difference in the capability to simulate drought and extreme event between GCMs is significant, and the uncertainty range with respect to GCMs is quite wide.

In summary, most downscaled rainfalls can reasonably reproduce observed monthly areal rainfall series in both calibration period and validation period, but a majority of downscaled rainfalls perform poorly when they come to droughts and extreme rainfalls. A further research task will be to improve the simulation accuracy of drought and extreme event to reduce risk in water resource management.

Acknowledgements This research is supported by National Natural Science Foundation of China (51079098) and Major Program of National Natural Science Foundation of China (40730632).

REFERENCES

- Cavazos, T. & Hewitson, B. C. (2005) Performance of NCEP variables in statistical downscaling of daily precipitation. *Clim. Res.* **28**, 95–107.
- Chiew, F. H. S., Kirono, D. G. C., Kent, D. M., Frost, A. J., Charles, S. P., Timbal, B., Nguyen, K. C. & Fu, G. (2010) Comparison of runoff modelled using rainfall from different downscaling methods for historical and future climates. *J. Hydrol.* **387**(1–2), 10–23.
- Chiew, F. H. S., Teng, J., Vaze, J. & Kirono, D. G. C. (2009) Influence of global climate model selection on runoff impact assessment. *J. Hydrol.* **379** (1–2), 172–180.

- Cleveland, W. S. (1979) Robust locally weighted regression and smoothing scatterplots. *J. Am. Stat. Assoc.* **74** (368), 829–836.
- Cleveland, W. S. & Devlin, S. J. (1988) Locally weighted regression: an approach to regression analysis by local fitting. *J. Am. Stat. Assoc.* **83**(403), 596–610.
- Edwards, D. C. & McKee, T. B. (1997) Characteristics of 20th century drought in the United States at multiple time scales. *Fort Collins Climatology Report*.
- Frich, P., Alexander, L. V., Della-Marta, P., Gleason, B., Haylock, M., Klein Tank, A. M. G. & Peterson, T. (2002) Observed coherent changes in climatic extremes during the second half of the 20th century. *Clim. Res.* **19**, 193–212.
- Ghosh, S. & Mujumdar, P. P. (2008) Statistical downscaling of GCM simulations to streamflow using relevance vector machine. *Adv. Water Res.* **31**(1), 132–146.
- Harpham, C. & Wilby, R. L. (2005) Multi-site downscaling of heavy daily precipitation occurrence and amounts. *J. Hydrol.* **312**(1–4), 235–255.
- Hewitson, B. C. & Crane, R. G. (1996) Climate downscaling: techniques and application. *Clim. Res.* **7**, 85–95.
- IPCC (2007) *Climate Change 2007: The Physical Basis*. Cambridge University Press, Cambridge, UK.
- Khan, M. S., Coulibaly, P. & Dibikey, Y. (2006) Uncertainty analysis of statistical downscaling methods. *J. Hydro.* **319**(1–4), 357–382.
- McKee, T. B. N., Doesken, J. & Kleist, J. (1993) The relationship of drought frequency and duration to time scales. In: *Eighth Conf. on Applied Climatology*. Anaheim, California, USA.
- Nicholls, N. & Alexander, L. (2007) Has the climate become more variable or extreme? Progress 1992–2006. *Progr. Phys. Geogr.* **31**, 77–87.
- Perkins, S. E., Pitman, A. J., Holbrook, N. J. & Mcaneney, J. (2007) Evaluation of the AR4 climate models' simulated daily maximum temperature, minimum temperature, and precipitation over Australia using probability density functions. *J. Climate* **20**, 4356–4376.
- Timbal, B., Fernandez, E. & Li, Z. (2009) Generalization of a statistical downscaling model to provide local climate change projections for Australia. *Environ. Model. Softw.* **24**(3), 341–358.
- Whitehead, P. G., Wilby, R. L., Butterfield, D. & Wade, A. J. (2006). Impacts of climate change on in-stream nitrogen in a lowland chalk stream: An appraisal of adaptation strategies. *Sci. Total Environ.* **365**(1–3), 260–273.
- Wilby, R. L., Dawson, C. W. & Barrow, E. M. (2002) SDSM – a decision support tool for the assessment of regional climate change impacts. *Environ. Model. Softw.* **17**(2), 145–157.
- Willmott, C. J. (1982) Some comments on the evaluation of model performance. *Bull. Am. Met. Soc.* **63**, 1309–1313.
- Zorita, E., Hughes, J. P., Lettemaier, D. P. & von Storch, H. (1995) Stochastic characterization of regional circulation patterns for climate model diagnosis and estimation of local precipitation. *J. Climate* **8**, 1023–1041.

